Journal of Engg. Research **Vol. 3 No. (3) September 2015** pp. 157-177

المحاكاة بالطرق العددية وتحليل انخفاض إنتاج الآبار الأفقية بواسطة الكسور المضاعفة في مكامن الغاز الصخري

، ***تينغ كوان كوه، **يونغ قانغ دون، ***يونغ وانغ، **ليهوي زانغ وكوانتانغ فانغ

*محطة أبحاث الدكتوراه، شركة نفط وغاز جنوب غرب سينوبك، وتشنغدو، سيتشوان، الصين

**مختبر الدولة للنفط وخزان الجيولوجيا واستغلال الغاز، جامعة جنوب الغرب للبترول، وتشنغدو، سيتشوان، الصين

***معهد بحوث تنمية الاستكشافات، شركة بترو جنوب غرب الصين ومجال النفط والغاز، وتشنغدو، الصين

الخلاصـة

طريقة تكاثر الآبار الأفقية المنكسرة يتم تطبيقها بكثافة في الآونة الأخيرة على نطاق واسع في إنتاج الغاز الصخري. ولذلك، فإن تحليل أداء هذه الطريقة مهم لاستغلال مكامن الغاز الصخري على نحو فعال. وهناك العديد من الأساليب التحليلية والعددية التي تم توظيفها لتحقيق الضغط المتغير أو زيادة إنتاجية الأبار بهذه الطريقة. ومع ذلك، فإن معظم هذه الأساليب ليست جيدة بما فيه الكفاية للتنبؤ بدقة سلوكيات تدفق السوائل من الغاز الصخري من خلال تطبيق القانون Darcy المعدل والنموذج المبسط للكسر. وتم اشتقاق هذه الدراسة استنادا إلى نموذج غاز المغبر ومعادلة Langmuir الحرارية، ومجموعة من معادلات التحكم، مع النظر في الامتزاز الغاز كثف إنتشارها، وتدفق الحمل الحراري. وتم بناء نموذج عددي من خلال تطبيق شبكات التنصيف المتعامدة مع توزيع لمعادلات التدفق. ويحقق هذا النموذج من آثار كسور الهيدروليكية والصخر الزيتي وخصائص المكمن على إنتاج الغاز. وأظهرت نتائج المحاكاة على: (1) إمتزاز الغاز الكثف يزيد من معدل الغاز ويطيل فترة التدفق، (2) الانتشارية والنفاذية أكبر في معدل الغاز وظهور مبكر لفترة مكون التدفق الخطي، (3) حجم أكبر لخزان المحاكاة، ويستمر لفترة أطول لتشكيل تدفق خطي. بالإضافة إلى ذلك، تشير هذه الدراسة إلى أن العدد الأمثل من الكسور والكسورمع الموصلية يؤدي إلى زيادة إنتاج البئر. ويعرض النموذج طريقه جديدة للمحاكاة عدديا وتوقع انخفاض الإنتاج في مكامن الغاز الصخري، وكذلك لتحسين التصميم الهيدروليكي لمتغيرات الكسر.

Numerical simulation and production decline analysis of multiply fractured horizontal wells in shale gas reservoirs

Tingkuan Cao*, **, Yonggang Duan**, Rong Wang***, Liehui Zhang** and Quantang Fang**

**Post-doctoral Research Station, SINOPEC Southwest Oil & Gas Company, Chengdu, Sichuan 610041, China*

***State Key Laboratory of Oil and Gas Reservoir Geology and Exploitation, Southwest Petroleum University, Chengdu 610500, Sichuan, PR China*

****Exploration and Development Research Institute, PetroChina Southwest Oil and Gasfield Company, Chengdu 610041, PR China*

***Corresponding author:caotingkuan@163.com*

ABSTRACT

Multiply fractured horizontal wells (MFHWs) have been widely applied into shale gas production recently. Thus, analyzing the performances of MFHWs is important for exploiting shale gas reservoirs effectively. There are various analytical and numerical methods, which have been employed to investigate pressure transient or well productivity of MFHWs. However, most of them are not good enough to accurately predict fluid flow behaviors of shale gas by applying the modified Darcy's law and oversimplified facture models.

Based on the Dusty-Gas Model and Langmuir isotherm equation, a set of governing equations, with the consideration of desorption of adsorbed gas, diffusion and convective flow is firstly derived in this work. Then a numerical model is constructed by applying the perpendicular bisection grids to discretize the flowing equations. This model is proposed to investigate the effects of hydraulic fractures and shale reservoir properties on gas production. The simulation results show that (1) desorption of adsorbed gas increases the gas rate and prolongs each flow period, (2) a larger diffusivity and matrix permeability result in a higher gas rate and an early appearance of compound linear flow period, (3) the larger the simulation reservoir volume is, the longer the formation linear flow lasts. In addition, this study also indicates that the optimized number of fractures and fractures with larger conductivity leads to increased well production. The proposed numerical model presents a new way to numerically simulate and predict the production decline of MFHWs in shale gas reservoirs, as well as to optimize hydraulic fracture parameters design.

Keywords: Adsorption-desorption; Dusty-Gas Model; multiply fractured horizontal well; production decline analysis; shale gas.

NOMENCLATURE

A, B	Coefficient matrix
A_{ij}	Area of the adjacent face between grid i and its neighbor grid j
B_{gi}	Volume factor under the initial condition (m^3/sm^3)
C	Molar concentration (mol/m^3)
c_{ti}	Total compressibility under the initial condition (Pa^{-1})
d_{fi}	Spacing of hydraulic fracture i (m)
d_i	Edge width of grid i (m)
d_{ij}	Distance between grid i and its neighbor grid j (m)
D_{ij}^e	Effective diffusion coefficient of component i in component j (m^2/s)
D_k	Knudsen diffusivity (m^2/s)
d_{pore}	Diameter of the nanopore (m)
F_{Ci}	Fracture conductivity of fracture (m^3)
h	Reservoir thickness or grid height (m)
k_0	Matrix permeability (m^2)
k_{fi}	Permeability of fracture i (m^2)
K_n	Knudsen number
L	Length of horizontal well (m)
l_{fi}	Length of hydraulic fracture i (m)
m	Number of components presenting in the system
M_g	Molecular weight of gas (kg/mol)
n	Time step
N	Molar flux ($mol \cdot m^{-2} \cdot s^{-1}$)
n_f	Fracture number
n_G	Grid number
N^k	Knudsen diffusive flux ($mol \cdot m^{-2} \cdot s^{-1}$)
N^v	Convective flux ($mol \cdot m^{-2} \cdot s^{-1}$)
$\dot{N}$	Amount generated in the control-volume in per unit time (mol/s)
p	Pressure of sample or reservoir (Pa)
$\overline{p}$	Average formation pressure (Pa)
p_0	Initial reservoir pressure (Pa)
p_i, p_j	Pressure of grid i, grid j (Pa)

p_L	Langmuir pressure of gas (Pa)
p_{wf}	Bottom hole flowing pressure (Pa)
q_a	Gas volume adsorbed in per unit solid volume at standard condition (sm^3/kg)
q_D	Dimensionless rate of a gas well
q_L	Langmuir gas volume (sm^3/kg)
q_{sc}	Produced gas rate at standard conditions (m^3/s)
q^*	Mass of adsorbed gas in per unit solid volume (kg/m^3)
R	Ideal gas constant (=8.314 $m^3 \cdot Pa \cdot K^{-1} \cdot mol^{-1}$)
r_{pore}	Characteristic length scale of the flow path (m)
r_w	Wellbore radius (m)
t	Actual production time (s)
T	System temperature (K)
t_D	Dimensionless production time
T_{ij}	Transmissibility between grid i and its neighbor grid j (m^3/s)
v	Iteration step
V_i	Volume of grid i (m^3)
V_{std}	Molar volume of an ideal gas at standard condition (=2.24×10^{-2} sm^3/mol)
w_{fi}	Width of hydraulic fracture i (m)
x_i, x_j	Mole fraction of component i, j
x_{fi}	Half length of the fracture i (m)
ϕ	Porosity of sample or porous media
ρ_s	Density of the porous sample (kg/m^3)
ρ_{sc}	Gas density at standard conditions (kg/m^3)
μ	Gas viscosity (Pa·s)
μ_{gi}	Viscosity of gas under the initial condition (Pa·s)
$\overline{\lambda}$	Gas molecular mean free path (m)
δp	Pressure difference (Pa)
∇p	Pressure gradient (Pa/m)
ADM	Advection-Diffusion Model
DGM	Dusty-Gas Model
MFHW	Multiply fractured horizontal well
PEBI	Perpendicular bisection

INTRODUCTION

Shale gas is an important unconventional gas resource, since it is of wide distribution and tremendous development potential. Unlike conventional gas resources, shale reservoir is featured by very low porosity and permeability, or more specifically, the porosity of shale matrix is usually lower than 10% and the permeability is generally in the micro- to nano-Darcy. These nanometer pores are the main storage space in shale gas reservoirs. In general, gas in shale is mainly stored as adsorbed gas and free gas. Therefore, these profound pore structures and multiple storage states of shale gas lead to complex transport mechanisms including adsorption-desorption, convective flow (Darcy flow or advection) and diffusion (Amann-Hildenbrand *et al*., 2012).

The impacts of adsorption-desorption on gas storage and transport have been reported by many researchers. According to Curtis (2002), the amount of adsorbed gas varies from shale to shale and accounts for 20% to 85% of the total reserves. Assuming that adsorbed gas obeyed Langmuir isotherm, various analytical models considering adsorption-desorption have been developed (Bumb & McKee, 1988; Mengal & Wattenbarger, 2011), and the calculated results displayed that adsorbed gas exhibited a negligible effect on production in early stages, but it mainly affected the late production period when the reservoir pressure had been decreased. Moreover, taking gas flow in shale nanopores into account, a numerical model was established to indicate that desorption of adsorbed gas would increase the cumulative production (Swami & Settari, 2012).

Except adsorption-desorption and convective flow, diffusion is another important transport mechanism, which influences the production of shale gas. So far, four types of models have been used to describe the transport of shale gas in the reservoirs. They are respectively Fick's law, Stefan-Maxwell equation, Advection-Diffusion Model (ADM) and Dusty-Gas Model (DGM), among which the most comprehensive approach is the DGM. Formulated by Evans *et al*. (1961, 1962), the DGM couples diffusion and advection based on Chapman-Enskog kinetic theory (Chapman & Cowling, 1970). Many investigators have compared the DGM with other models in detail, and they concluded that for shale matrix with pore-throat smaller than 1×10^{-6} m and with extremely low permeability, the DGM is preferred to describe gas transport through porous media (Cunningham & Williams, 1980; Mason & Malinauskas, 1983; Webb & Pruess, 2003).

MFHWs are widely applied into unconventional gas reservoirs. According to the pressure transient characteristics of MFHWs, three discrete flow periods are divided by Van Kruysdijk & Dullaert (1989), i.e. formation linear flow, compound formation linear flow and pseudo-elliptical flow. In order to study the productivity of MFHWs in shale reservoirs, many analytical and semi-analytical models were presented (Guo

& Yu, 2008; Medeiros *et al.*, 2008). However, only few of these models have taken adsorption-desorption and diffusion into proper consideration. Combined Cartesian grids with the local grid refinement technique, numerical simulators considering multiple flow mechanisms were developed to capture the accurate flow behaviors of fractures (Cheng, 2011; Freeman *et al*., 2013). While Cartesian grids could not efficiently describe the main wellbore and fractures of MFHWs, and the results would suffer from significant grid orientation effects. Compared with Cartesian grids, perpendicular bisection (PEBI) grids are more flexible and allow for a better grid construction near the wellbores and hydraulic fractures (An *et al*., 2012).

In order to describe the gas flow through shale matrix more comprehensively, a novel mathematical model is derived based on the DGM and Langmuir isotherm model. In the proposed model, the diffusive and convective fluxes are combined in the DGM, and the amount of desorption calculated by Langmuir isotherm is added to the mass conservation equation as the source/sink term. Then, based on EasyMesh code for PEBI grid generating, a numerical model for MFHWs is constructed by PEBI grid discretization. A fully implicit technique and Gauss-Seidel iteration method are applied to solve this model. Based on the established model, the performance characteristics of MFHWs in shale gas reservoirs can be predicted, and the hydraulic fracture parameters can be optimized to guide more efficient development of shale gas reservoirs.

MECHANISMS OF GAS FLOWING THROUGH SHALE GAS RESERVOIRS

The main transport mechanisms of gas flow through shale matrix are briefly summarized in this section. These mechanisms include desorption of adsorbed gas, diffusion and advection. Diffusion is a process where the gas molecules move from an area of high concentration to that of lower one. The main two types of diffusion are molecular and Knudsen diffusion. The difference between them is that molecular diffusion is dominated by molecule-molecule collisions, while Knudsen diffusion is molecule-wall collisions dominant. Molecular diffusion is most difficult mechanism to be properly defined (Webb, 1998). However, this paper focuses on single-phase gas flow, so the effect of molecular diffusion is not included.

Adsorption and desorption

According to the study of Fathi & Akkutlu (2009), adsorption-desorption is an important migration mechanism in the porous media. As constant formation temperature is usually assumed in reservoir development, the amount of adsorbed gas can be adequately described by Langmuir isotherm equation:

$$q_a = \frac{q_L p}{p_L + p} \tag{1}$$

Equation (1) can also be expressed in the following form

$$q^* = \frac{\rho_s M_g}{V_{std}} q_a = \frac{\rho_s M_g}{V_{std}} \frac{q_L p}{p_L + p} \tag{2}$$

Knudsen diffusion

In the free-molecule region, the molecular mean free path is larger than the characteristic dimension of the porous medium, so molecule-wall interactions dominate over molecule-molecule interactions and Knudsen diffusion obviously occurs (Webb, 1998). The Knudsen number K_n is defined to identify and divide flow regimes in porous media (Freeman et al., 2011), which is given by

$$K_n = \frac{\overline{\lambda}}{r_{pore}} \tag{3}$$

When Knudsen number is less than 0.01, the gas flow obeys Darcy's law. While Knudsen number is higher than this value, the effective permeability should be corrected for the effect of diffusion.

Knudsen diffusion is significant in shale matrix with small pores (smaller than a few micrometers) and at low pressures (Freeman *et al*., 2011). The net flux in Knudsen diffusion is proportional to the gradient of the molecular density (Cunningham & Williams, 1980).

$$N^k = -D_k \frac{\partial C}{\partial z} \tag{4}$$

In order to further evaluate the influence of Knudsen diffusion on gas flow process, Javadpour *et al*. (2007) proposed the relation for estimating the Knudsen diffusion coefficient, that is

$$D_k = \frac{d_{pore}}{3} \sqrt{\frac{8RT}{\pi M_g}} \tag{5}$$

Based on the physical interpretation of Klinkenberg correction proposed by Javadpour *et al*. (2007) and the empirical relation between effective pore-throat radius and permeability as well as porosity (Karniadakis & Beskok, 2002), the diffusivity is given by

$$D_k = \frac{4 c_0 k_0}{2.81708 \sqrt{k_0/\phi}} \sqrt{\frac{\pi RT}{2M_g}} \tag{6}$$

where c_0 is a constant value at 1.0 .

Convective flow

Convective flow is the fluid flow driven by pressure gradient in porous media. The convective flux can be described by Darcy's law (ignoring the effect of gravity),

$$N^v = -\frac{k_0}{\mu}\frac{p}{RT}\nabla p \tag{7}$$

FLOW MODEL FOR MFHWS IN SHALE RESERVOIRS

In order to further analyze the impacts of transport mechanisms for shale gas on flow characteristics, the PEBI grids are introduced to describe the numerical model and simulate the flow process of MFHWs. The PEBI grids, used in this study, are constructed based on a numerical generation procedure which is referred largely to the open source code called EasyMesh (available at the website http://web. mit. edu/ easymesh_v1.4/ www/ easymesh. html).

Model descriptions and assumptions

The schematic of the simulation model used in this study is shown in Figure 1, and the mathematical model for a MFHW in a shale gas reservoir is derived based on the following assumptions:

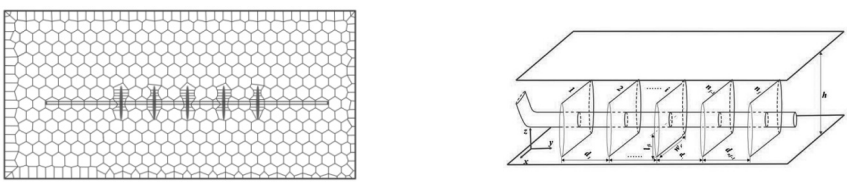

Fig. 1 (a). Top view **Fig. 1 (b).** Lateral view

Fig. 1. The schematic of a MFHW in a shale gas reservoir

1. A single-layer shale reservoir is considered, with both the top and bottom boundaries closed and the lateral boundaries impermeable. The formation is homogenous and isotropic with the same thickness h and matrix permeability k_0. Before production, reservoir pressure, equaling to the initial pressure p_0, is also homogeneously distributed.
2. A MFHW with length of L is centrally located in the bounded rectangle reservoir, and all vertical transverse hydraulic fractures (a total of n_f) are assumed to penetrate the formation completely, each fracture with length of l_{fi} (i=1, 2, …, n_f), width of w_{fi}, spacing of d_{fi}, and permeability of k_{fi} (see Figure 1(b)).
3. The MFHW is under a constant bottom-hole pressure. Gas flow in horizontal wellbore is assumed to be infinitely conductive. The fracture grids, which are

intersected by horizontal wellbore, are constant pressure grids, and the other fracture grids are taken as grids with high permeability (that is, fracture permeability is far greater than matrix permeability).

4. The solving variables of grids which are intersected by horizontal wellbore are gas rate, while the variables to be solved of other grids are pressure.
5. Since the surface gas rate of each fracture is q_i (i=1, 2, …, n_f), the total rate of the MFHW is the sum of all the fractures rate.
6. Simulated fluid is single gaseous phase of methane in an isothermal flow. And the gas properties, such as viscosity, change with reservoir pressure dropping.
7. Gravity and capillary force are negligible. The fluid flow in vertical direction is not considered.

For typical MFHWs in shale gas reservoirs, the aperture of hydraulic fractures is on the order of millimeters, and the permeability of hydraulic fractures is about a few Darcy. While the permeability in shale matrix is usually lower than micro-Darcy, and the grid size is as large as tens of meters. If the above actual values are used in the simulation, the numerical stability and convergence will be affected by the difference between hydraulic fractures and shale matrix. Thus, we treat the fracture as possessing a fixed conductivity as described in Equation (8), and reduce the fracture permeability by magnifying the width of fracture appropriately.

$$F_{Ci} = k_{fi} \cdot w_{fi} \tag{8}$$

In this study, we assume the fracture with width of 5×10^{-3} m and with permeability of 0.5×10^{-12} m^2, thus the fracture conductivity is 2.5×10^{-15} m^3. The simulated grid size of shale matrix is 50 m, while the aperture of hydraulic fracture is magnified to 2.5 m considering the stability and convergence of simulation, and the fracture permeability reduces to 10^{-15} m^2 relatively.

Flow equation

When gas flowing in the porous media is described as the DGM, the effect of convection caused by pressure gradient and the impact of diffusion caused by concentration difference are all taken into consideration.

Based on the equation of state for an ideal gas, the flow equation can be expressed in the form of pressure gradient. The general form of the DGM for multi-components is given by

$$\sum_{j=1,j\neq i}^{m} \frac{x_i N_j - x_j N_i}{D_{ij}^e} - \frac{N_i}{D_k} = \frac{p}{RT}\nabla x_i + (1+\frac{k_0 p}{\mu D_k})\frac{x_i \nabla p}{RT} \tag{9}$$

where the subscript *i* or *j* represents component of gas. In Equation (9), the first term on the left hand side represents molecular diffusion, and the second term accounts for Knudsen diffusion.

For a single component gas system, the molecular diffusion is not considered, and Equation (9) can be simplified as

$$N = -(D_k + \frac{k_0 p}{\mu})\frac{\nabla p}{RT} \tag{10}$$

Mass conservation equation

Figure 2 shows a schematic of PEBI grids. Here, *i* is the gridblock number; *j* is a neighbor of matrix grid *i*; d_i is width of the edge between grid *i* and grid *j*; d_{ij} is the distance between grid *i* and grid *j*; and *h* is the height of grid *i*. A_{ij} is area of the adjacent face between grid *i* and grid *j*, thus, $A_{ij}=d_i h$.

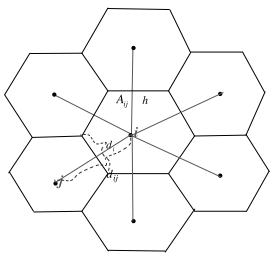

Fig. 2. Schematic of PEBI grids

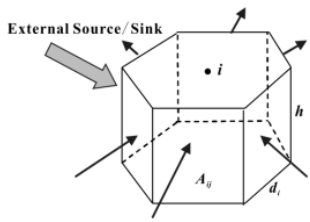

Fig. 3. Three-dimensional schematic of grid *i*

As shown in Figure 3, when the PEBI grid *i* is selected as control-volume, the sum of gas flux flowing from its adjacent grids into grid *i* and the increased or decreased gas flux in grid *i* through the sink or source, equals to the increased flux in grid *i* at unit time. Based on mass conservation law, the governing equation in the grid *i* can be obtained, i.e.

$$-\sum_j NA_{ij} + \dot{N} = V_i \frac{\partial(\phi C)}{\partial t} \tag{11}$$

where *N* is the molar flux between grid *i* and its adjacent grid *j*. $\dot{N}$ (mol/s) is the amount of component generated in the control-volume in per unit time, including production and desorption.

For the selected grid *i*, $\dot{N}$ can be expressed as

$$\dot{N} = \frac{\rho_{sc} q_{sc}}{M_g} - \frac{V_i}{M_g} \cdot \frac{\partial[(1-\phi)q^*]}{\partial t} \tag{12}$$

The first term on the right hand side represents the produced gas flux, and the second term accounts for the desorbed gas flux, which is opposite to the amount of adsorbed gas.

Flow differential equation

Combining the DGM of single component gas with equation of mass conservation, the solution of concentration is transformed into the solution of pressure distribution according to equation of state for an ideal gas. Assuming the porosity of shale is constant, the flow differential equation for single-phase gas system is obtained, i.e.

$$\sum_j \left(\frac{D_k A_{ij}}{RT} + \frac{k_0 p A_{ij}}{\mu RT}\right) \cdot \nabla p + \frac{\rho_{sc} q_{sc}}{M_g} - \frac{V_i p_L (1-\phi) q^*}{M_g p (p_L + p)} \cdot \frac{\partial p}{\partial t} = \frac{V_i \phi}{RT} \cdot \frac{\partial p}{\partial t} \tag{13}$$

In Equation (13), the permeability k_0, Langmuir pressure p_L and Langmuir volume q_L can be measured by experiments, viscosity μ can be obtained by theoretical calculation at a certain pressure and temperature, and Knudsen diffusivity D_k can be calculated by Equation (7).

Initial and boundary conditions

According to the hypothesis of mathematical model, the outer boundary is impermeable and the bottom-hole pressure of inner boundary is constant.

$$\frac{\partial p}{\partial x} = 0 \tag{14}$$

$$p_{wf}\Big|_{r=r_w} = C_1 \tag{15}$$

At original time (t=0), pressure of the shale gas reservoir is described as

$$p(x, y, t)\Big|_{t=0} = p_0 \tag{16}$$

DESCRIPTION OF NUMERICAL MODEL

Since Equation (13) is nonlinear due to the inconstant gas viscosity, numerical method is more favorable to solve the series of equations compared with analytical method. Based on the model assumptions, the flow differential Equation (13) can be discretized based on PEBI grids, which can be divided into grids of constant pressure and grids of non-constant pressure. And the results are as follows:

For grids of non-constant pressure,

$$\sum_j T_{ij}^{n+1} (p_j^{n+1} - p_i^{n+1}) - \frac{\Gamma_i^{n+1}}{\Delta t} (p_i^{n+1} - p_i^n) = \frac{V_i \phi}{\Delta t} (p_i^{n+1} - p_i^n) \tag{17}$$

And for grids of constant-pressure,

$$\sum_j T_{ij}^{n+1} (p_j^{n+1} - p_i^{n+1}) + \frac{\rho_{sc} q_{sc} RT}{M_g} = 0 \tag{18}$$

where the transmissibility is defined as $T_{ij}=\frac{D_k A_{ij}}{d_{ij}}+\frac{k_0 A_{ij} p}{\mu d_{ij}}$, and the definition of Γ_i is $\Gamma_i=\frac{V_i p_L(1-\phi)RTq^*}{M_g p(p_L+p)}$.

In Equations (17) and (18), the coefficients and variables are calculated at (n+1) time step except for p_i^n when approximating time derivative. A fully implicit technique is applied to construct the coefficient matrix. The coefficients and variables are expanded using the first-order of Taylor series expansion, neglecting the second-order items. Then, rearranging yields:

For grids of non-constant pressure (shale matrix grids),

$$\sum_j T_{ij}^{(v)n+1}\cdot\delta p_j^{(v+1)n+1}-[\sum_j T_{ij}^{(v)n+1}+\frac{V_i\phi}{\Delta t}+\frac{\Gamma_i^{(v)n+1}}{\Delta t}+\frac{1}{\Delta t}\frac{\partial\Gamma_i}{\partial p_i}\Big|_{n+1}^{(v)}\cdot(p_i^{(v)n+1}-p_i^n)]\cdot\delta p_i^{(v+1)n+1}+\sum_j\frac{\partial T_{ij}}{\partial p_{ij}}\Big|_{n+1}^{(v)}(p_j^{(v)n+1}-p_i^{(v)n+1})\cdot\delta p_{ij}^{(v+1)n+1}$$
$$=\frac{V_i\phi}{\Delta t}(p_i^{(v)n+1}-p_i^n)-\sum_j T_{ij}^{(v)n+1}(p_j^{(v)n+1}-p_i^{(v)n+1})+\frac{\Gamma_i}{\Delta t}\Big|_{n+1}^{(v)}(p_i^{(v)n+1}-p_i^n) \tag{19}$$

For grids of constant-pressure (well grids),

$$\sum_j T_{ij}^{(v)n+1}\cdot\delta p_j^{(v+1)n+1}+\sum_j\frac{\partial T_{ij}}{\partial p_{ij}}\Big|_{n+1}^{(v)}(p_j^{(v)n+1}-p_i^{(v)n+1})\cdot\delta p_{ij}^{(v+1)n+1}+\frac{\rho_{sc}RT}{M_g}\cdot q_{sc}=-\sum_j T_{ij}^{(v)n+1}(p_j^{(v)n+1}-p_i^{(v)n+1}) \tag{20}$$

Here, the superscripts v, v+1 represent iteration step, and the superscripts n, n+1 denote time step. δp_{ij} is calculated by upstream weighted method, i.e.

$$\delta p_{ij}=\begin{cases}\delta p_j & p_j>p_i\\ \delta p_i & p_j<p_i\end{cases} \tag{21}$$

The number of simulation grids is assumed to be n_G, and the number of fractures is n_f, then the number of constant-pressure grids (the grids which fractures are intersected by the horizontal well) is n_f, and the number of non-constant pressure grids is (n_G–n_f). Thus, the following matrix can be established as

$$A\cdot X=B \tag{22}$$

Where

$$X=(\delta p_1,\delta p_2,\delta p_i\cdots,\delta p_{n_G-n_f},q_1,q_2,q_{n_f})^T \tag{23}$$

and

$$\delta p_i=p_i^{(v+1)n+1}-p_i^{(v)n+1} \tag{24}$$

If grid i belongs to [1, n_G–n_f] (grids of non-constant pressure), grid j is the neighbor of

grid i, and grid k is not adjacent with grid i, then coefficient matrix can be expressed as

$$\begin{cases} A_{ii} = -[\sum_j T_{ij}^{(v)n+1} + \dfrac{V_i\phi}{\Delta t} + \dfrac{\Gamma_i^{(v)n+1}}{\Delta t} + \dfrac{1}{\Delta t}\dfrac{\partial \Gamma_i}{\partial p_i}\Big|_{n+1}^{(v)} \cdot (p_i^{(v)n+1} - p_i^n)] \\ A_{ij} = \sum_j T_{ij}^{(v)n+1} + \sum_j \dfrac{\partial T_{ij}}{\partial p_{ij}}\Big|_{n+1}^{(v)} (p_j^{(v)n+1} - p_i^{(v)n+1}) \\ A_{ik} = 0 \\ B_i = \dfrac{V_i\phi}{\Delta t}(p_i^{(v)n+1} - p_i^n) - \sum_j T_{ij}^{(v)n+1}(p_j^{(v)n+1} - p_i^{(v)n+1}) + \dfrac{\Gamma_i}{\Delta t}\Big|_{n+1}^{(v)}(p_i^{(v)n+1} - p_i^n) \end{cases}, \quad p_j^{(v)n+1} > p_i^{(v)n+1} \tag{25}$$

or

$$\begin{cases} A_{ii} = \sum_j \dfrac{\partial T_{ij}}{\partial p_{ij}}\Big|_{n+1}^{(v)} (p_j^{(v)n+1} - p_i^{(v)n+1}) - [\sum_j T_{ij}^{(v)n+1} + \dfrac{V_i\phi}{\Delta t} + \dfrac{\Gamma_i^{(v)n+1}}{\Delta t} + \dfrac{1}{\Delta t}\dfrac{\partial \Gamma_i}{\partial p_i}\Big|_{n+1}^{(v)} \cdot (p_i^{(v)n+1} - p_i^n)] \\ A_{ij} = \sum_j T_{ij}^{(v)n+1} \\ A_{ik} = 0 \\ B_i = \dfrac{V_i\phi}{\Delta t}(p_i^{(v)n+1} - p_i^n) - \sum_j T_{ij}^{(v)n+1}(p_j^{(v)n+1} - p_i^{(v)n+1}) + \dfrac{\Gamma_i}{\Delta t}\Big|_{n+1}^{(v)}(p_i^{(v)n+1} - p_i^n) \end{cases}, p_i^{(v)n+1} > p_j^{(v)n+1} \tag{26}$$

If grid i belongs to $[n_G - n_f + 1, n_G]$ (grid of constant-pressure), grid j is the neighbor of grid i, and grid k is not adjacent with grid i, then coefficient matrix can be expressed as

$$\begin{cases} A_{ii} = \dfrac{\rho_{sc} RT}{M_g} \\ A_{ij} = \sum_j T_{ij}^{(v)n+1} + \sum_j \dfrac{\partial T_{ij}}{\partial p_j}\Big|_{n+1}^{(v)} (p_j^{(v)n+1} - p_i) \\ A_{ik} = 0 \\ B_i = -\sum_j T_{ij}^{(v)n+1}(p_j^{(v)n+1} - p_i^{(v)n+1}) \end{cases} \tag{27}$$

Since the coefficient matrix of Equations (25), (26) and (27) are sparse and strictly diagonally dominant, Gauss-Seidel Iteration Method is adopted to solve the matrix. Thus pressure and flux can be obtained, and convergence condition is as follows

$$\max\left| p_i^{(v+1)n+1} - p_i^{(v)n+1} \right| \le 0.001Pa, \qquad i = 1,2,\ldots,n_G \tag{28}$$

The gas rate of a MFHW at a constant bottom-hole pressure condition can be

calculated by above methods. For the convenience of further analysis, the dimensionless form of gas rate and production time can be defined as

$$q_D = \frac{\mu_{gi} B_{gi}}{2\pi k_0 h(\bar{p} - p_{wf})} q_{sc} \tag{29}$$

$$t_D = \frac{k_0 t}{\phi \mu_{gi} c_{ti} x_f^{\ 2}} \tag{30}$$

RESULTS AND DISCUSSION

Simulation parameters

Based on the developed model, numerical simulation is conducted to study the production decline law and its factors of the MFHW in shale gas reservoirs. The basic data used in the simulating are shown in Table 1.

Table 1. Basic parameters used in numerical simulation

Parameter	Value	Parameter	Value
Simulation reservoir volume V, m^3	1000×500×30	Knudsen diffusivity D_k, m^2/s	1×10^{-8}
Initial reservoir pressure P_i, Pa	2×10^7	Number of fractures n_f	5
Button hole pressure P_{wf}, Pa	1.2×10^7	Fracture spacing d_f, m	100
Porosity ϕ, f	0.05	Fracture length l_f, m	100
Reservoir temperature T, K	333.15	Length of horizontal well L, m	900
Formation depth H, m	2000	Fracture width w_f, m	5×10^{-3}
Permeability of shale matrix k_0, m^2	1×10^{-19}	Conductivity of fracture F_C, m^3	2.5×10^{-15}
Gas density at standard conditions ρ_{sc}, kg/m^3	0.717	Langmuir volume q_L, m^3/kg	0.01
Molar mass of methane M_g, kg/mol	0.016	Langmuir pressure P_L, Pa	7.5×10^6

Production decline analysis

Based on the basic parameters shown in Table 1, the simulation results of dimensionless gas rate versus dimensionless time for the MFHW in a shale gas reservoir are shown in Figure 4. From Figure 4, it can be found that a MFHW in shale gas reservoirs has an extraordinarily high gas rate as well as a fast decline speed in the initial stage, but the decrease speed tends to slow down, as a result, a MFHW has a prolonged production time.

To study the production history of the MFHW more carefully, the whole production process is divided into five periods according to the research results of Van Kruysdijk *et al*. (1989) and Freeman *et al*. (2013). The first period is linear flow in hydraulic fractures, as shown in Figure 5(a). And the second one is formation linear flow period

which fluid flows from shale matrix into fractures linearly (see Figure 5(b)). With the pressure wave continuously spreading away from fractures, these linear pressure pulses interfere with each other, and the transition period is observed. As indicated in Figure 5(c), pressure wave gradually changes its orientation with the gas produced around fractures, and the gas flows into hydraulic fractures in linear manners. Thus, the compound linear flow period occurs only when the linear flow also appears in the formation. Because of the extra-low permeability of shale reservoirs, gas well goes through a long production decline period before pseudo-radial flow appears, and the transition period between compound linear flow and pseudo-radial flow is called pseudo-elliptical flow (see Figure 5(d)).

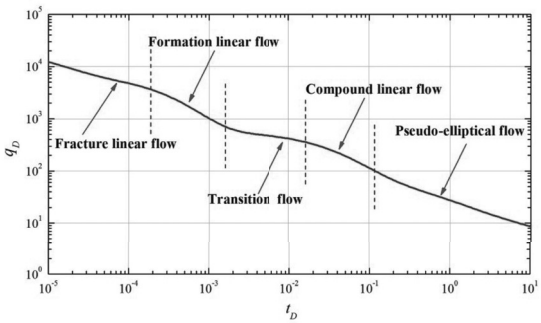

Fig. 4. Dimensionless gas rate versus dimensionless production time of the MFHW

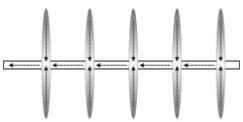

Fig. 5 (a). linear flow in fractures

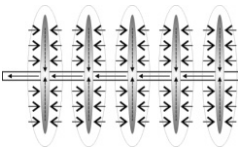

Fig.5 (b). formation linear flow

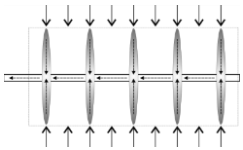

Fig. 5 (c). compound linear flow

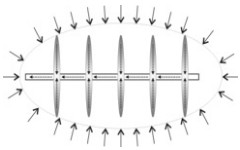

Fig. 5 (d). pseudo-elliptical flow

Fig. 5. Schematic diagrams of flow regimes of the MFHW in a shale gas reservoir

Sensitivity analysis of production performance

The numerical model is used to evaluate the influence of parameters, including desorption of adsorbed gas, Knudsen diffusivity (D_k), matrix permeability (k_0), number of hydraulic fractures (n_f), fracture spacing (d_f), fracture length (l_f), fracture

conductivity (F_C) and simulation reservoir volume (V) on production performance of the MFHW in shale gas reservoirs.

To investigate the impact of adsorbed gas on dimensionless production, a case with no adsorbed gas is simulated and compared to that with adsorbed gas. The results are shown in Figure 6. It is seen that desorption of adsorbed gas would help to increase gas rate and prolong each production period of the MFHW. That means adsorption-desorption is an important mechanism for the gas storage and migration, and the effects of adsorption-desorption must be taken into consideration when simulating the performance of MFHWs in shale gas reservoirs.

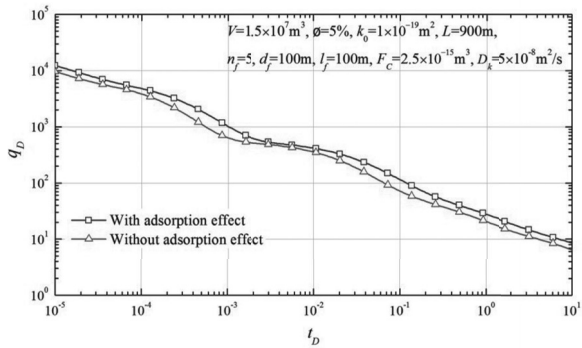

Fig. 6. Effect of gas desorption on dimensionless production curves of the MFHW

Figure 7 demonstrates the influence of Knudsen diffusion coefficient D_k on the production of the MFHW. The results shown in Figure 7 indicate that Knudsen diffusion mainly influences the middle to late stage of a gas well production, while the early stage is less affected. The larger the D_k is, the higher the gas rate is. The earlier the compound linear flow and pseudo-elliptical flow stage appears, the slower the gas rate declines in later period. The reason for this is that with the increase of Knudsen diffusivity, the capacity of gas supply is stronger and gas converges from shale matrix into fractures more quickly, which results in a high gas rate and low production decline speed.

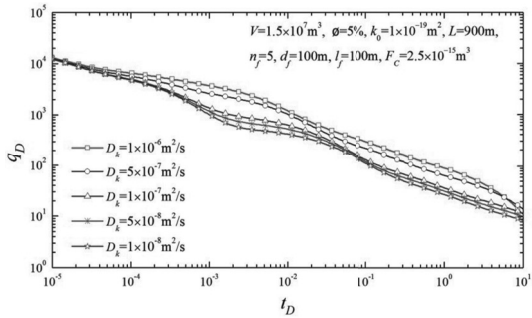

Fig. 7. Effect of diffusion coefficient on dimensionless rate of the MFHW

Figure 8 shows the dimensionless production decline curves of the MFHW at different matrix permeability k_0, 1×10^{-17} m^2, 1×10^{-18} m^2, 1×10^{-19} m^2, 1×10^{-20} m^2, respectively. From Figure 8, it can be seen that k_0 has a greater influence on the rate in later production stage than in the early stage. With the increase of k_0, the flow rate is higher but declines more quickly, the formation linear flow period becomes shorter, and compound linear flow and pseudo-elliptical flow emerge earlier.

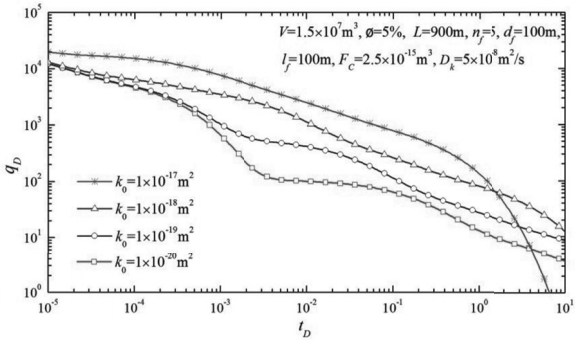

Fig. 8. Effect of matrix permeability on dimensionless rate of the MFHW

Figure 9 denotes the effect of the number of fractures (n_f) on dimensionless rate of a MFHW in shale gas reservoirs. As is shown in Figure 9, gas rate rises with the increase of n_f, but the growth of gas rate slows down if fracturing treatment scale continues increasing. By comparing the gas rate at different n_f, conclusions can be drawn that the more the n_f is, the higher the rate is. But with the further increase of n_f, the contribution of a single fracture to total gas rate declines gradually. So, there is an optimal fracture number for the MFHW in shale gas formation, and seven is the probably favorable fractures number for hydraulic fracturing stimulation in this study.

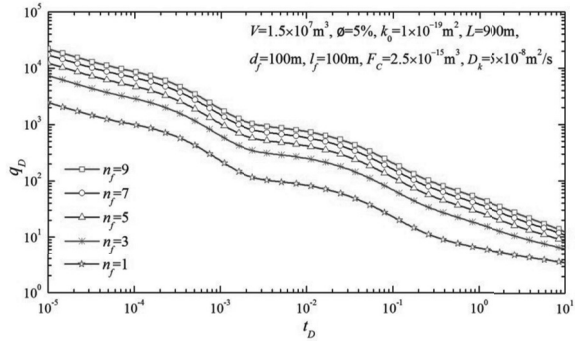

Fig. 9. Effect of number of fractures on dimensionless gas rate curves of the MFHW

Figure 10 indicates that the gas rate curves of the MFHW with different fracture spacing (d_f). The fractures are presumed to be equally spaced and have the same properties. From Figure 10, it can be found that d_f mainly affects gas rate of late-time

while almost has little effect on the early- and intermediate-time production. With the same number of fractures, the larger the d_f is, the longer the compound linear flow lasts, and the production declines more slowly, when entering into pseudo-elliptical flow period. It is because of the fact that increasing d_f will shift fracture interference among linear flow backward.

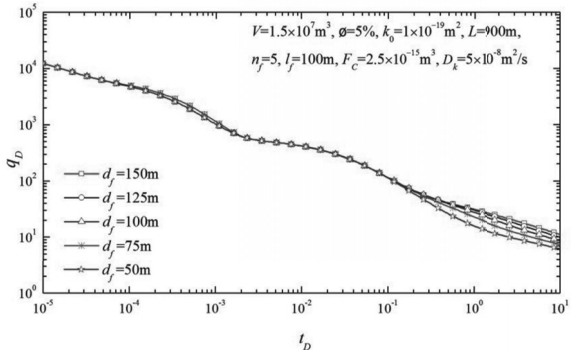

Fig. 10. Effect of different fracture spacing on dimensionless gas rate of the MFHW

Keeping the other simulation data constant, the fracture length (l_f) changes from 50m to 150m with an interval of 25m, and the simulating results are shown in Figure 11. It can be noted that with the increase of l_f, the formation linear flow period lasts longer and gas rate declines more slowly. However, the rate difference of gas wells with different l_f tends to be slight, when it comes into compound linear flow period. The reason for the above phenomenon is that l_f mainly affects the early-time rate, while the production of shale gas well in late-time is controlled by shale matrix properties, such as permeability and diffusivity.

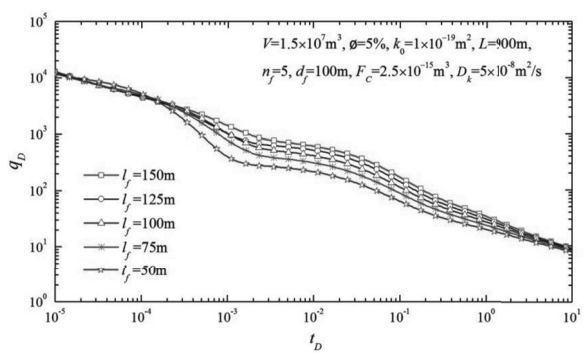

Fig. 11. Effect of fracture length on dimensionless production of the MFHW

Figure 12 depicts the trends of dimensionless rate curves of shale gas well at different facture conductivity (F_C), 2.5×10^{-15} m^3, 2.5×10^{-16} m^3, 2.5×10^{-17} m^3, 2.5×10^{-18} m^3, respectively. It can be seen that with all the other parameters constant, a larger F_C of hydraulic factures leads to a higher initial rate. With the production of shale gas,

the effect of F_C on gas rate decreases, and ultimately the rate of wells with different F_C will merge.

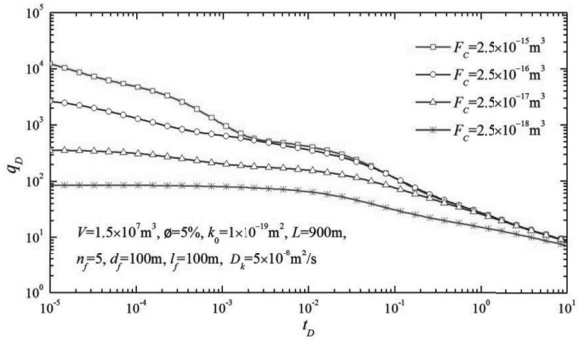

Fig. 12. Effect of facture conductivity on dimensionless production of the MFHW

Figure 13 illustrates the production performance of the MFHW affected by simulation reservoir volume (V). It can be seen that a larger V leads to a higher gas rate, slower production decline, longer duration of formation linear flow period and later transition toward compound linear flow.

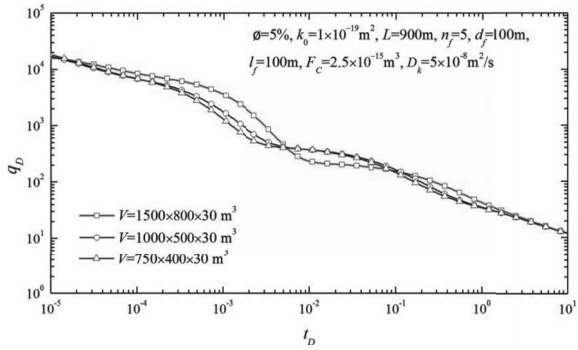

Fig. 13. Effect of simulation reservoir volume on dimensionless rate of the MFHW

CONCLUSIONS

A novel simulation model for a MFHW in shale gas reservoirs is developed using the DGM, Langmuir isotherm theory and PEBI grids discretization methods. Compared with previous models, the new model takes several mechanisms into proper consideration, including desorption of adsorbed gas, Knudsen diffusion and convection flow. Hence, the new numerical model can be used to predict the production decline rule and optimize the hydraulic fracture parameters of the MFHW in shale gas reservoirs.

Dimensionless production curves for the MFHW in shale gas reservoirs are established, and five main flow periods, namely fracture linear flow, formation linear

flow, transition flow, compound linear flow and pseudo-elliptical flow period, are observed according to the characters of the curve shapes.

Adsorption-desorption is an important transport and migration mechanism for shale gas. Desorption of adsorbed gas in shale matrix increases the gas rate and prolongs the duration of each production period.

Diffusion coefficient D_k and matrix permeability k_0 mainly affect the appearing time of compound linear flow, a larger D_k and k_0 result in a higher gas rate and an early appearance of compound linear flow period. And with the increase of simulation reservoir volume V, the gas production increases and formation linear flow period lasts longer.

Fracture parameters have important effects on early-time production of a shale gas well. The more number of fractures, the longer fracture length, and the higher fracture conductivity, will result in a higher initial gas rate. The simulation results also indicate that the number of fractures for a MFHW should be optimized to increase gas rate.

ACKNOWLEDGMENTS

The authors are grateful for financial support from the National Science Fund for Distinguished Young Scholars of China (Grant No. 51125019) and the National Program on Key Fundamental Research Project (973 Program, Grant No. 2013CB228005).

REFERENCES

Amann-Hildenbrand, A., Ghanizadeh, A. & Krooss, B.M. 2012. Transport properties of unconventional gas systems. Marine and Petroleum Geology **31**(1): 90-99.

An, Y., Wu, X. & Gao, D. 2012. On the use of PEBI grids in the numerical simulations of two-phase flows in fractured horizontal wells. Computer Modeling in Engineering & Science **89**(2): 123-141.

Bumb, A.C. & McKee, C.R. 1988. Gas-well testing in the presence of desorption for coalbed methane and Devonian shale. SPE Formation Evaluation **3**(1): 179-185.

Chapman, S. & Cowling, T.G. 1970. The mathematical theory of non-uniform gases: an account of the kinetic theory of viscosity, thermal conduction and diffusion in gases. Cambridge University Press, Cambridge.

Cheng, Y. 2011. Pressure transient characteristics of hydraulically fractured horizontal shale gas wells. Paper SPE 149311 presented at SPE Eastern Regional Meeting, Columbus, Ohio, USA.

Cunningham, R.E. & Williams, R.J.J. 1980. Diffusion in gases and porous media. Plenum press, New York.

Curtis, J.B. 2002. Fractured shale-gas systems. American Association of Petroleum Geologists bulletin 86(11): 1921-1938.

Evans III, R.B., Watson, G.M. & Mason, E.A. 1961. Gaseous diffusion in porous media at uniform pressure. Journal of Chemical Physics **35**: 2076-2083.

Evans III, R.B., Watson, G.M. & Mason, E.A. 1962. Gaseous diffusion in porous media. II. Effect of pressure gradients. Journal of Chemical Physics **36**: 1894-1902.

Fathi, E. & Akkutlu, I.Y. 2009. Matrix heterogeneity effects on gas transport and adsorption in coalbed and shale gas reservoirs. Transport in Porous Media **80**(2): 281-304.

Freeman, C.M., Moridis, G.J. & Blasingame, T.A. 2011. A numerical study of microscale flow behavior in tight gas and shale gas reservoir systems. Transport in Porous Media **90**: 253-268.

Freeman, C.M., Moridis, G., Ilk, D. & Blasingame, T.A. 2013. A numerical study of performance for tight gas and shale gas reservoir systems. Journal of Petroleum Science and Engineering **108**: 22-39.

Guo, B. & Yu, X. 2008. A simple and accurate mathematical model for predicting productivity of multifractured horizontal wells. Paper SPE 114452 presented at CIPC/SPE Gas Technology Symposium 2008 Joint Conference, Calgary, Alberta, Canada.

Javadpour, F., Fisher, D. & Unsworth, M. 2007. Nanoscale gas flow in shale gas sediments. Journal of Canadian Petroleum Technology **46**(10): 55-60.

Karniadakis, G.E. & Beskok, A. 2002. Micro flows: Fundamentals and simulation. Springer–Verlag, New York.

Mason, E.A. & Malinauskas, A.P. 1983. Gas transport in porous media: The dusty-gas model. Elsevier, Amsterdam, Netherlands.

Medeiros, F., Ozkan, E. & Kazemi, H. 2008. Productivity and drainage area of fractured horizontal wells in tight gas reservoirs. SPE Reservoir Evaluation & Engineering **11**(05): 902-911.

Mengal, S.A. & Wattenbarger, R.A. 2011. Accounting for adsorbed gas in shale gas reservoirs. SPE Paper 141085 presented at SPE Middle East Oil and Gas Show and Conference, Manama, Bahrain.

Swami, V. & Settari, A. 2012. A pore scale gas flow model for shale gas reservoir. SPE Paper 155756 presented at SPE Americas Unconventional Resources Conference, Pittsburgh, Pennsylvania.

Van Kruysdijk, C. & Dullaert, G.M. 1989. A boundary element solution to the transient pressure response of multiple-fractures horizontal wells. Paper presented at the 1st European Conference on the Mathematics of Oil Recovery, Cambridge, England.

Webb, S.W. 1998. Gas-phase diffusion in porous media-evaluation of an advective-dispersive formulation and the dusty-gas model for binary mixtures. Journal of Porous Media **1**: 187-199.

Webb, S.W. & Pruess, K. 2003. The use of Fick's law for modeling trace gas diffusion in porous media. Transport in Porous Media **51**: 327-341.

Submitted: 13-12-2014
Revised: 18-03-2015
Accepted: 08-04-2015